Three-body model study of $A=6-7$ hypernuclei: Halo and skin structures

Emiko Hiyama and Masayasu Kamimura
Department of Physics, Kyushu University, Fukuoka 812, Japan

Toshio Motoba
Laboratory of Physics, Osaka Electro-Communication University, Neyagawa, Osaka 572, Japan

Taiichi Yamada
Laboratory of Physics, Kanto Gakuin University, Yokohama 236, Japan

Yasuo Yamamoto
Physics Section, Tsuru University, Tsuru, Yamanashi 402, Japan

(Received 2 January 1996)

Low-lying states of $A=6$ hypernuclear doublets ($^{6}_{\Lambda}$He and $^{6}_{\Lambda}$Li) and $A=7$ triplets ($^{7}_{\Lambda}$He, $^{7}_{\Lambda}$Li, and $^{7}_{\Lambda}$Be) are studied with an accurate three-body model calculation in which all the rearrangement Jacobian coordinates are equally taken into account. Since most of the hypernuclear states concerned are weakly bound states, focus is placed on the binding energies with respect to the particle breakup thresholds and on the density distributions in the surface and exterior regions. With the $\alpha+\Lambda+N$ model, the observed binding energies of the ground states of $^{6}_{\Lambda}$He and $^{6}_{\Lambda}$Li are well reproduced. $^{6}_{\Lambda}$He is found to have a three-layer structure of the matter distribution: the α nuclear core, a Λ skin, and a neutron halo. The $A=7$ hypernuclei are shown to be well described with the $^{5}_{\Lambda}$He $+$ $N+N$ model. Using a realistic NN interaction, the correlation between the valence nucleons is fully taken into account; this is essentially important to make the *proton-rich* three-body system $^{7}_{\Lambda}$Be $=$ $^{5}_{\Lambda}$He $+$ $p+p$ bound although none of the two-body subsystems is bound. The observed binding energies of $^{7}_{\Lambda}$Li and $^{7}_{\Lambda}$Be are well reproduced, and energies are predicted for $^{7}_{\Lambda}$He whose core nucleus is a neutron halo nucleus, ^{6}He. We discuss the validity of the assumption of frozen deuterons adopted in the previous $\alpha+d+\Lambda$ models for the $T=0$ states of $^{7}_{\Lambda}$Li.

PACS number(s): 21.80.+a, 21.10.Dr, 21.10.Gv, 21.45.+v

I. INTRODUCTION

One of the purposes of hypernuclear physics is to study the new dynamical features induced by the Λ particle. In light p-shell hypernuclei, the remarkable role of the Λ particle has been pointed out in Refs. [1,2]: that the Λ participation gives rise to more bound states and the appreciable contraction of the system (this stabilization is called the ''gluelike'' role of the Λ). This feature of light hypernuclei has been studied mostly in systems composed of a stable nucleus and a Λ particle. Recently, in light nuclei near the neutron drip line, interesting phenomena concerning the neutron halo have been observed [3]. If a Λ particle is added to such a halo nucleus, a very weakly bound system, the resultant hypernucleus will become substantially stable against the neutron decay. Thanks to the gluelike role of the Λ particle, there is a new chance to produce a hypernuclear neutron (proton) halo state if the core nucleus has a weakly unbound (resonant) state with an appropriate energy above the particle decay threshold.

In this way, hypernuclei have the interesting possibility of extending the neutron (proton) drip line from that obtained in ordinary nuclei. A typical example is $^{6}_{\Lambda}$He. Though the core nucleus ^{5}He is unbound by 0.89 MeV above the $\alpha+n$ breakup threshold, the ground state of $^{6}_{\Lambda}$He becomes barely bound by 0.17 MeV below the $^{5}_{\Lambda}$He $+$ n threshold. The observed Λ binding energy of 4.18 MeV [4] is mostly exhausted to bind the $\alpha+\Lambda$ subsystem [$B_{\Lambda}^{\rm expt}(^{5}_{\Lambda}\mathrm{He}) = 3.12$ MeV] [5], and the coupling between the subsystem and the valence neutron is very weak. Thus $^{6}_{\Lambda}$He is expected to have a neutron halo structure around the $^{5}_{\Lambda}$He core. This picture of $^{6}_{\Lambda}$He $=$ $^{5}_{\Lambda}$He $+$ n seems to be a dominating structure when we characterize the structure of the $^{6}_{\Lambda}$He $=$ $\alpha+\Lambda+n$ system. The same picture $^{5}_{\Lambda}$He $+$ p is expected to hold for $^{6}_{\Lambda}$Li, the other member of the isospin-doublet hypernuclei with $A=6$. The first aim of this paper is to study the structure of the $^{6}_{\Lambda}\mathrm{He}=\alpha+\Lambda+n$ system with the coupled-rearrangement-channel method [6–8] which has been successful in describing the halo structure of neutron-rich light nuclei. As a result, we found that the ground state of $^{6}_{\Lambda}$He has a three-layer structure of the matter distribution, composed of the α core, a Λ skin, and a neutron halo, which is characterized by a dominant structure of $^{5}_{\Lambda}$He $+$ n with 95% probability. This result shows that the $^{5}_{\Lambda}$He $+$ n picture is very good to describe the low-lying states of $^{6}_{\Lambda}$He. We also study the structure of the $^{6}_{\Lambda}\mathrm{Li}=\alpha+\Lambda+p$ system. This picture should be applicable to the $A=7$ hypernuclei by taking the $^{5}_{\Lambda}$He $+$ $N+N$ model.

Another typical example is $^{7}_{\Lambda}$Be, as for the change of the (proton) drip line due to the gluelike role of the added Λ particle. While the nucleus ^{6}Be is located at 1.37 MeV above the $\alpha+p+p$ breakup threshold, the hypernucleus $^{7}_{\Lambda}$Be is bound by 0.67 MeV below the $^{5}_{\Lambda}$He $+$ $p+p$ threshold [cf.

$B_{\Lambda}^{\rm expt}({}^{7}_{\Lambda}{\rm Be}) = 5.16$ MeV [9]]. Since the ${}^{5}_{\Lambda}{\rm He} + p$ subsystem is unbound by 0.59 MeV [cf. $B_{\Lambda}^{\rm expt}({}^{6}_{\Lambda}{\rm Li}) = 4.50$ MeV [10]], the p-p correlation in the ${}^{5}_{\Lambda}{\rm He} + p+p$ system plays an essentially important role in making ${}^{7}_{\Lambda}{\rm Be}$ bound. It is interesting to note that this ${}^{7}_{\Lambda}{\rm Be} = {}^{5}_{\Lambda}{\rm He} + p+p$ hypernucleus is considered to be the only *proton-rich* Borromean system so far reported in nuclei and hypernuclei (a three-body system in which the total system is bound but none of the two-body subsystems are bound is called a Borromean [11]). The second purpose of the present paper is then to investigate the mechanism of binding of the proton-rich hypernucleus ${}^{7}_{\Lambda}{\rm Be}$. We shall make the ${}^{5}_{\Lambda}{\rm He} + p+p$ three-body calculation with sufficient accuracy. We treat fully the correlations between the valence protons using a realistic NN interaction (Bonn A [12]) since the protons are considered to be mostly located outside the ${}^{5}_{\Lambda}{\rm He}$ core because of their weak coupling with ${}^{5}_{\Lambda}{\rm He}$. As a result, we found that the observed binding energy of ${}^{7}_{\Lambda}{\rm Be}$ is satisfactorily reproduced by the model. Therefore, since binding energies of the remaining members of the isospin-triplet hypernuclei with $A=7$, ${}^{7}_{\Lambda}{\rm He}$ and ${}^{7}_{\Lambda}{\rm Li}$ ($T=1$), have not been observed yet, it is of particular interest to apply the same ${}^{5}_{\Lambda}{\rm He} + N+N$ model to the hypernuclei and predict their binding energies.

${}^{6}{\rm He}$ is known to be a typical neutron halo nucleus in the light p-shell region [13]; the two-neutron separation energy is only 0.975 MeV. This nucleus is well described by an $\alpha+n+n$ three-body model [8,11,14–16]. Though the $\alpha+n$ system is unbound, the n-n correlation of the valence neutrons makes the three-body system stable against neutron emission. The Λ participation in the bound state of such a halo nucleus should result in a more stable ground state of the hypernucleus. The shell-model calculations of ${}^{7}_{\Lambda}{\rm He}$ [17,18] indicate that the ground state ($1/2^{+}$) and the excited doublet states ($3/2^{+}$,$5/2^{+}$) are located below the ${}^{5}_{\Lambda}{\rm He} + n+n$ threshold if the calculated energy of the ground state of ${}^{6}{\rm He}$ is adjusted to the observed energy with respect to the $\alpha+n+n$ threshold. However, in order to investigate the binding energies rigorously, it is desirable to employ a theoretical framework which takes into account the neutron breakup thresholds explicitly and is suitable for describing weakly bound states. The present ${}^{5}_{\Lambda}{\rm He} + n+n$ model for ${}^{7}_{\Lambda}{\rm He}$ and the $\alpha+n+n$ one for ${}^{6}{\rm He}$ are quite useful for this purpose. We shall predict the binding energy of this *neutron-rich* hypernucleus ${}^{7}_{\Lambda}{\rm He}$ and discuss the spatial extension of the valence neutrons in these states.

The $T=1,0^{+}$ state of the ${}^{6}{\rm Li}$ nucleus at $E_x = 3.56$ MeV, which is located at only 0.14 MeV below the $\alpha+n+p$ threshold, has been noted to have a proton halo [19]. The addition of a Λ particle to the ${}^{6}{\rm Li}$ nucleus will stabilize this $T=1$ state, while it makes the next excited $T=1$ state with 2^{+} at $E_x = 5.37$ MeV come down to the energy region of a proton (neutron) halo candidate in ${}^{7}_{\Lambda}{\rm Li}$. This mechanism will be investigated with the ${}^{5}_{\Lambda}{\rm He} + n+p$ model, too.

It is well known that calculation of the Λ spin-doublet states in ${}^{7}_{\Lambda}{\rm Li}$ is very useful to get information on the spin-spin term of the ΛN interaction. The calculated energy splitting depends on both the model and the effective ΛN interaction employed. The energy splitting of the ground-state spin doublet $1/2^{+}$-$3/2^{+}$ has been predicted as 0.44–0.79 MeV by shell-model calculations [17,18] in which the model space is restricted to the $(0s)^4(0p)^2 0s_{\Lambda}$ configuration only. $\alpha+d+\Lambda$ cluster-model calculations [1,20] predicted the energy as 1.1–1.33 MeV. We are now ready to improve the latter model by removing the frozen deuteron assumption, since the probability of the deuteron clusterization is only 65% in the ground state of the ${}^{6}{\rm Li}$ nucleus (cf. Sec. IV B) and further distortion of the deuteron is expected in ${}^{7}_{\Lambda}{\rm Li}$ due to the gluelike role of the Λ particle. It is noted that the assumption of the frozen deuteron possibly gives rise to an overestimation of the spin-spin interaction between the Λ particle and the n-p pair. Since high-resolution experiments are expected in the near future for the energy splitting of the spin-doublet states, it is highly desirable to perform less model-dependent calculations of these states. We consider that a better approach to the low-lying $T=0$ states of ${}^{7}_{\Lambda}{\rm Li}$ is to adopt the ${}^{5}_{\Lambda}{\rm He} + n+p$ model so as to take the full n-p correlation into account. Taking this framework without assuming a deuteron cluster, it is possible to investigate both the $T=0$ and $T=1$ states of ${}^{7}_{\Lambda}{\rm Li}$ on an equal footing.

In order to study these loosely coupling states mentioned above, it is very useful to take all three kinds of the Jacobian coordinates explicitly and employ the corresponding three-body Gaussian basis functions [6–8]. The method to calculate the three-body matrix elements of the complicated interactions such as realistic NN interactions (Bonn A, etc.) has been developed by the two of the present authors (E.H. and M.K.) [8]. These methods are used throughout the present work.

In Sec. II, the structure of the isospin-doublet hypernuclei ${}^{6}_{\Lambda}{\rm He}$ and ${}^{6}_{\Lambda}{\rm Li}$ is investigated with the $\alpha+\Lambda+N$ three-body model. On the basis of the very weak coupling between the ${}^{5}_{\Lambda}{\rm He}$ cluster and the valence nucleon, we propose the ${}^{5}_{\Lambda}{\rm He} + N+N$ picture for the $A=7$ Λ hypernuclei. In Sec. III, this model is formulated and applied to the isospin-triplet levels of ${}^{7}_{\Lambda}{\rm He}$, ${}^{7}_{\Lambda}{\rm Li}$, and ${}^{7}_{\Lambda}{\rm Be}$. Section IV is devoted to the study of the low-lying $T=0$ states of ${}^{7}_{\Lambda}{\rm Li}$ with the same model. Emphasis is placed on the splitting of the Λ spin-doublet states and the degree of the deuteron clusterization in the presence of the gluelike role of the Λ particle. A summary is given in Sec. V.

II. ${}^{6}_{\Lambda}$He AND ${}^{6}_{\Lambda}$Li

A. Model

We assume that the hypernuclei ${}^{6}_{\Lambda}{\rm He}$ and ${}^{6}_{\Lambda}{\rm Li}$ are composed of an α cluster, a valence nucleon (N), and a Λ particle (Fig. 1). The core nucleus α is considered to be an inert core and to have the $(0s)^4$ configuration, $\Phi(\alpha)$. The Pauli principle between the valence nucleon and the core nucleons is taken into account by the orthogonality condition model (OCM) [21], as the valence nucleon's wave function should be orthogonal to that of the core nucleon. Thus we solve the $\alpha+\Lambda+N$ three-body problem with the total Hamiltonian given by

$$H = T + V_{\alpha N}(\mathbf{r}_1) + V_{\alpha\Lambda}(\mathbf{r}_2) + V_{\Lambda N}(\mathbf{r}_3) + V_{\rm Pauli}. \quad (2.1)$$

Here, T is the kinetic-energy operator and V_{ab} is the interaction between the constituent particles a and b. The OCM projection operator $V_{\rm Pauli}$ is represented by

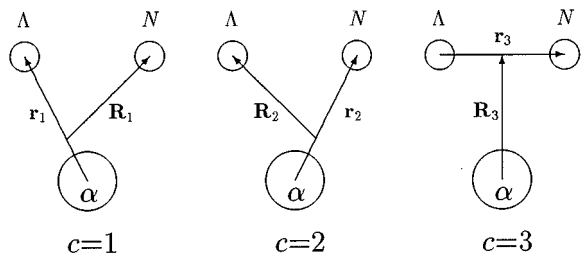

FIG. 1. Jacobian coordinates of the three rearrangement channels adopted for the $\alpha+\Lambda+N$ model of ${}^{6}_{\Lambda}$He and ${}^{6}_{\Lambda}$Li.

$$V_{\rm Pauli}=\lim_{\lambda\to\infty}\lambda|\phi_{0s}(\mathbf{r}_{N\alpha})\rangle\langle\phi_{0s}(\mathbf{r}'_{N\alpha})| \quad (N=n \text{ or } p), \tag{2.2}$$

which excludes the amplitude of the Pauli forbidden state $\phi_{0s}(\mathbf{r})$ from the three-body total wave function [22]. The Gaussian size parameter b in ϕ_{0s} is taken to be $b=1.358$ fm as in the literature [1]. In actual calculations, the strength λ for $V_{\rm Pauli}$ is taken to be 10^6 MeV, which is large enough to push up the unphysical forbidden states in the very-high-energy region while keeping the physical states unchanged. The usefulness of this Pauli operator method of the OCM has been verified in many cluster-model calculations of light nuclei [8,15,16].

In order to solve accurately the three-body problem, we employ the coupled-rearrangement-channel Gaussian basis variational method which was developed by two of the present authors (E.H. and M.K.) and their collaborators [6–8]. The total wave function of the $A=6$ hypernucleus ${}^{6}_{\Lambda}$Z is described as a sum of the amplitudes of the three rearrangement channels (Fig. 1) in the LS coupling scheme:

$$\Psi_{JM}({}^{6}_{\Lambda}Z)=\sum_{c=1}^{3}\sum_{I,S}\Phi(\alpha)[\phi_I^{(c)}(\mathbf{r}_c,\mathbf{R}_c) \times[\chi_{1/2}(\Lambda)\chi_{1/2}(N)]_S]_{JM}, \tag{2.3}$$

where $\phi_I^{(c)}$ is the spatial-coordinate amplitude with angular momentum I and the χ's are the spin wave functions coupled to spin S. We then expand each $\phi_I(\mathbf{r},\mathbf{R})$ in terms of Jacobian-coordinate Gaussian basis functions [6,7] which are known to be suited for describing both short-range correlations and long-range tail behavior:

$$\phi_{IM}(\mathbf{r},\mathbf{R})=\sum_{l,L}\sum_{n=1}^{n_{\max}}\sum_{N=1}^{N_{\max}}C_{nlNL}^{(I)}r^l R^L e^{-(r/r_n)^2}e^{-(R/R_N)^2} \times[Y_l(\hat{\mathbf{r}})\otimes Y_L(\hat{\mathbf{R}})]_{IM}. \tag{2.4}$$

Here, the Gaussian range parameters are taken to be of geometrical progression,

$$r_n=r_{\min}a^{n-1} \quad (n=1\sim n_{\max}),$$
$$R_N=R_{\min}a^{N-1} \quad (N=1\sim N_{\max}). \tag{2.5}$$

TABLE I. The angular-momentum model space of the three-body basis functions and the Gaussian range parameters employed for the ground state of ${}^{6}_{\Lambda}$He. Lengths are given in units of fm. The c_i distinguishes the channels of Jacobian coordinates shown by Fig. 1.

c	l	L	I	S	$n_{\max}$	$r_{\min}$	$r_{\max}$	$N_{\max}$	$R_{\min}$	$R_{\max}$
c_1	0	1	1	0	10	0.2	10.0	10	0.5	15.0
c_1	0	1	1	1	10	0.2	10.0	10	0.5	15.0
c_2	1	0	1	0	15	0.5	20.0	10	0.5	10.0
c_2	1	0	1	1	15	0.5	20.0	10	0.5	10.0
c_3	0	1	1	0	8	0.2	10.0	8	0.5	12.0
c_3	0	1	1	1	8	0.2	10.0	8	0.5	12.0

This prescription has been found to be very useful in optimizing the ranges with a small number of free parameters together with high accuracy [6–8].

The eigenenergies of the Hamiltonian and the wave function coefficients C are determined by the Rayleigh-Litz variational method. In the procedure of optimizing the parameters of the basis functions, it is very useful to pay attention to the following point: Since the ground states of ${}^{6}_{\Lambda}$He and ${}^{6}_{\Lambda}$Li are located very close to the ${}^{5}_{\Lambda}$He + N breakup threshold, the states are composed dominantly of the loosely coupled ${}^{5}_{\Lambda}$He + N system, especially in the asymptotic region. It is then effective to employ the configurations of the channel $c=1$ as the most important ones to describe the wave functions of such states. In this sense, the present approach is more suitable for those systems than the previous work [1,20] where only the basis functions of the channel $c=2$ were taken into account. The optimized parameters are listed in Table I (cf. the discussions in Secs. II B and II C for the dominant role of the channel $c=1$).

As for the ΛN interaction $V_{\Lambda N}$, we employ a one-range Gaussian (ORG) interaction [1,20]; it is given by the following form with no exchange term:

$$V_{\Lambda N}=V_{\Lambda N}^0(1+\eta\boldsymbol{\sigma}_\Lambda\cdot\boldsymbol{\sigma}_N)e^{-(r/\beta)^2} \tag{2.6}$$

with $V_{\Lambda N}^0=-38.19$ MeV, $\beta=1.034$ fm, and $\eta=-0.1$. The range β is chosen to be equivalent to the two-pion exchange Yukawa, and the potential strength $V_{\Lambda N}^0$ was determined so as to reproduce the experimental Λ binding energy in ${}^{5}_{\Lambda}$He ($B_\Lambda=3.12$ MeV) [5]. The strength η of the spin-spin term was taken to reproduce the splitting of the 0^+ and 1^+ states of ${}^{4}_{\Lambda}$H (${}^{4}_{\Lambda}$He) within the ^{3}H + Λ (^{3}He + Λ) cluster model [5]. The $\alpha\Lambda$ interaction $V_{\alpha\Lambda}$ is obtained by folding $V_{\Lambda N}$ into the nucleon density of the α particle with the spin-spin term vanishing.

Careful attention should be paid to the αN interaction since the Λ binding energy is measured from the energy $E_{\alpha N}$ of the lowest resonant state of the $\alpha+N$ system above the $\alpha+N$ breakup threshold. In the calculation for ${}^{6}_{\Lambda}$He in Ref. [1], the authors obtained $E_{\alpha n}=1.13$ MeV within the bound-state approximation. We found, however, that an accurate αN scattering calculation leads to $E_{\alpha n}=0.59$ MeV. The error of 0.54 MeV has a direct effect on the value of $B_\Lambda({}^{6}_{\Lambda}$He) which is measured from $E_{\alpha N}$. Furthermore, this αN interaction used in Ref. [1] does not satisfactorily repro-

TABLE II. Calculated energies of the low-lying states of ${}^{6}_{\Lambda}$He and ${}^{6}_{\Lambda}$Li together with those of the corresponding states of ^{5}He and ^{5}Li. The energies E are measured from the $\alpha+N$ threshold for the $A=5$ nuclei and from the $\alpha+\Lambda+N$ threshold for $A=6$ hypernuclei. The energies in parentheses are measured from the ${}^{5}_{\Lambda}$He + N threshold. The rms distances $\overline{r_{\alpha-N}}$, $\overline{r_{\alpha-\Lambda}}$, and $\overline{r_{\Lambda-N}}$ are also listed for the bound state.

	^{5}He	${}^{6}_{\Lambda}$He		^{5}Li	${}^{6}_{\Lambda}$Li	
J	$3/2^-$	1^-	2^-	$3/2^-$	1^-	2^-
E (MeV)	0.89	−3.37	−3.01	1.97	−2.54	− 2.15
		(−0.25)	(0.11)		(0.58)	(0.97)
$E^{\rm expt}$ (MeV)	0.89	−3.29		1.97	−2.53	
		(−0.17)			(0.59)	
B_Λ (MeV)		4.26	3.94		4.51	4.09
$B_\Lambda^{\rm expt}$ (MeV)		4.18			4.50	
$\overline{r_{\alpha-n}}$ (fm)		5.22				
$\overline{r_{\alpha-\Lambda}}$ (fm)		2.57				
$\overline{r_{\Lambda-n}}$ (fm)		5.54				

duce the low-energy αN scattering data. In the following calculation, therefore, we employ the αN interaction of Kanada *et al.* [23] proposed on the basis of a microscopic $\alpha+N$ model calculation. This interaction reproduces precisely the αN phase shifts of the $3/2^-$, $1/2^-$, and $1/2^+$ partial waves at low energies; it is composed of parity-dependent central and spin-orbit parts. The αn and αp interactions are the same except for the Coulomb term which is constructed by folding the pp Coulomb potential into the proton density of the α particle.

B. Results

The calculated energies of ${}^{6}_{\Lambda}$He and ${}^{6}_{\Lambda}$Li are summarized in Table II. The observed Λ binding energies are well reproduced. Since the 1^- ground state of ${}^{6}_{\Lambda}$He is bound only by 0.17 MeV with respect to the ${}^{5}_{\Lambda}$He + n threshold, the channel $c=1$ is essentially important to describe the weakly bound neutron. In fact, the energy calculated with the basis functions of the channel $c=1$ alone almost reproduces the experimental value within a small angular-momentum space of $l,L\leqslant 1$, whereas use of the channel $c=2$ alone does not give any bound state even if l and L are both extended to 2.

The binding energy of the valence neutron in ${}^{6}_{\Lambda}$He is weak enough to show a halo structure. In order to demonstrate it, we introduce the monopole density of the valence neutron, $\rho_n(r_2)$, as a function of the relative distance r_2 from the α particle (cf. Fig. 1), which is obtained by integrating over the other Jacobian coordinate $\mathbf{R}_2$ and the angular part of $\mathbf{r}_2$:

$$\rho_n(r_2)=\int |\Psi({}^{6}_{\Lambda}\mathrm{He})|^2 d\mathbf{R}_2 d\hat{\mathbf{r}}_2/4\pi. \tag{2.7}$$

Let us define the rms distance of the valence neutron from the α particle, $\overline{r_{\alpha-n}}$, by

$$\overline{r_{\alpha-n}}=\left[4\pi\int r_2^2\rho_n(r_2)r_2^2 dr_2\right]^{1/2}. \tag{2.8}$$

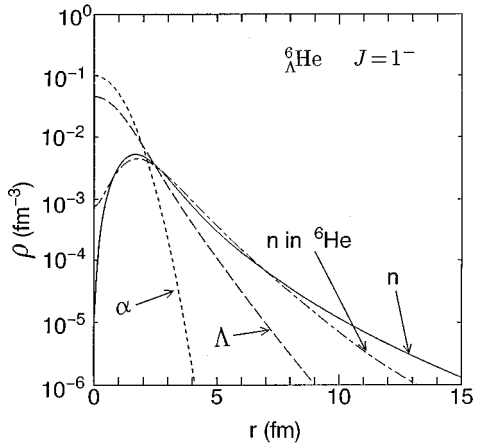

FIG. 2. Density distribution of the valence neutron, ρ_n, in the ground state of ${}^{6}_{\Lambda}$He together with those of the Λ particle, ρ_Λ, and a single nucleon in the α core. The radius r is measured from the c.m. of the α core.

Similarly, we give the density $\rho_\Lambda(r_1)$ and the rms distances $\overline{r_{\alpha-\Lambda}}$ and $\overline{r_{\Lambda-n}}$.

The calculated densities ρ_n and ρ_Λ of ${}^{6}_{\Lambda}$He are illustrated in Fig. 2 together with the density of a single nucleon in the α core. In the same figure we also insert the density of the valence halo neutron in ^{6}He as a function of the distance between the neutron and the α particle. It is remarkable to find a clear halo of the valence neutron density $\rho_n(r_2)$ in ${}^{6}_{\Lambda}$He at the tail region. The extension of the neutron density in ${}^{6}_{\Lambda}$He, namely, the neutron halo, is more evident than that in ^{6}He. To confirm the neutron halo structure, we list the rms distances $\overline{r_{\alpha-n}}$, $\overline{r_{\alpha-\Lambda}}$, and $\overline{r_{\Lambda-n}}$ in Table II. It is interesting to note that the size of the valence neutron's distribution (5.22 fm) in ${}^{6}_{\Lambda}$He is larger than that in the ^{6}He nucleus (4.5 fm) [8,15], which is a typical neutron halo nucleus. The density of the Λ particle is shorter ranged than that of the valence neutron, but is extended significantly away from the α core. We call it the Λ skin. We can say that there are *three* layers of matter distribution in the hypernucleus ${}^{6}_{\Lambda}$He, namely, the α core, a Λ skin, and a neutron halo.

C. ${}^{5}_{\Lambda}$He clusterization in ${}^{6}_{\Lambda}$He and ${}^{6}_{\Lambda}$Li

In the hypernuclei ${}^{6}_{\Lambda}$He and ${}^{6}_{\Lambda}$Li, the Λ particle is bound to the α particle mostly in the $0s_\Lambda$ orbit, while the valence nucleon is very loosely coupled to the $\alpha+\Lambda$ subsystem. As mentioned above, the role of the channels $c=2$ and 3 has been proved to be very small. In fact, in the ground state of ${}^{6}_{\Lambda}$He (1^-), the probability of finding the $\alpha+\Lambda$ subsystem in its ground state (${}^{5}_{\Lambda}$He) amounts to 95%. In addition, the calculated rms distance between α and Λ in ${}^{6}_{\Lambda}$He is 2.57 fm, showing that the $\alpha+\Lambda$ subsystem does not change greatly from the free ${}^{5}_{\Lambda}$He, which has the α-Λ distance 2.79 fm. Therefore it is a good approximation to consider that ${}^{6}_{\Lambda}$He (${}^{6}_{\Lambda}$Li) is composed of a ${}^{5}_{\Lambda}$He cluster and a loosely coupled neutron (proton). On the contrary, it does not work satisfactorily to approximate the $A=6$ Λ hypernucleus to be a dicluster system with a ^{5}He (^{5}Li) nucleus and a Λ particle. The present investigation of the ${}^{6}_{\Lambda}$He (${}^{6}_{\Lambda}$Li) structure pro-

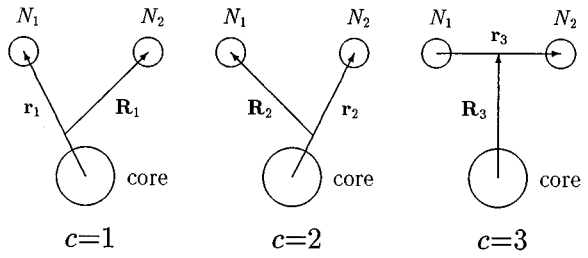

FIG. 3. Jacobian coordinates of the three rearrangement channels of the ''core''$+N+N$ model. Here, ''core'' is α for the $A=6$ nuclei and ${}^{5}_{\Lambda}$He for the $A=7$ hypernuclei.

vides us with a useful model to describe the $A=7$ Λ hypernucleus as a three-body system consisting of the ${}^{5}_{\Lambda}$He core and two valence nucleons in spite of the four units $(\alpha+\Lambda+N+N)$. Therefore the N-N correlation in the ${}^{5}_{\Lambda}$He-cluster field will play an important role in determining the structure of the $A=7$ hypernuclei. This will be studied in the following sections.

III. ${}^{7}_{\Lambda}$He , ${}^{7}_{\Lambda}$Li ($T=1$), AND ${}^{7}_{\Lambda}$Be

On the basis of the study of ${}^{6}_{\Lambda}$He and ${}^{6}_{\Lambda}$Li in the previous section, here we employ the ${}^{5}_{\Lambda}$He $+$ $N+N$ model for the $A=7$ hypernuclei. Before going to the hypernuclei, we investigate the $A=6$ nuclei, ^{6}He, ^{6}Li ($T=1$), and ^{6}Be, to which the Λ particle will be injected. Since the $A=6$ nuclei are studied with the $\alpha+N+N$ model, we can discuss the structure of $A=6$ nuclei and $A=7$ hypernuclei from the same viewpoint of three-body dynamics.

A. The model for $A=6$ nuclei

We assume that $A=6$ nuclei are composed of two valence nucleons (N_1 and N_2) and an α inert core (Fig. 3). The Pauli principle is taken into account by assuring that the valence nucleon's wave function is orthogonal to the core nucleon wave function in the same manner as in the $\alpha+\Lambda+N$ model in Sec. II. The total Hamiltonian is then written as

$$H=T+V_{\alpha N_1}(\mathbf{r}_1)+V_{\alpha N_2}(\mathbf{r}_2)+V_{N_1N_2}(\mathbf{r}_3)+V_{\text{Pauli}}, \tag{3.1}$$

where $V_{\alpha N}$ and V_{NN} include the Coulomb interaction for $N=p$. $V_{\alpha N}$ and V_{Pauli} are completely the same as in Sec. II for ${}^{6}_{\Lambda}$He and ${}^{6}_{\Lambda}$Li. Since the interaction between the α core and the valence nucleons is rather weak and the nucleons are moving mostly outside the α core under the Pauli condition, we treat fully the correlation between valence nucleons with the use of a realistic NN interaction. The Bonn A potential [12] is adopted for this reason; our previous study of ^{6}He [8] showed that use of other realistic potentials gives rise to very similar results for the nucleus.

According to the coupled-rearrangement-channel variational method [6–8], the total wave function of the $A=6$ nucleus, $\Psi_{JM}({}^{6}Z)$, is expressed as a sum of the amplitudes of the three rearrangement channels $c=1-3$ in Fig. 3:

TABLE III. The angular-momentum model space of the three-body basis functions and the Gaussian range parameters employed for the $J=0^+$ states of ^{6}He, ^{6}Li ($T=1$), and ^{6}Be. See also comments for Table I.

c	l	L	I	S	$n_{\max}$	$r_{\min}$	$r_{\max}$	$N_{\max}$	$R_{\min}$	$R_{\max}$
$c_{1,2}$	0	0	0	0	12	0.5	7.0	12	0.5	7.0
$c_{1,2}$	1	1	0	0	12	0.5	7.0	12	0.5	7.0
$c_{1,2}$	1	1	1	1	12	0.5	7.0	12	0.5	7.0
c_3	0	0	0	0	12	0.1	7.0	12	0.5	7.0
c_3	1	1	1	1	12	0.1	7.0	12	0.5	7.0

$$\Psi_{JM}({}^{6}Z)=\sum_{c=1}^{3}\sum_{I,S}\Phi(\alpha)[\phi_I^{(c)}(\mathbf{r}_c,\mathbf{R}_c) \times[\chi_{1/2}(N_1)\chi_{1/2}(N_2)]_S]_{JM}. \tag{3.2}$$

The notations are the same as in Eq. (2.3). In the case of ^{6}He and ^{6}Be, Ψ_{JM} is antisymmetrized for exchange between N_1 and N_2; hence the following condition should hold: $\phi_I^{(1)}=-\phi_I^{(2)}$ for $S=1$, while $\phi_I^{(1)}=\phi_I^{(2)}$ for $S=0$. As for ^{6}Li, the valence neutron and proton are treated as different particles. The isospin is slightly mixed between $T=0$ and 1 due to the Coulomb interaction and the n-p mass difference, but, for simplicity, we refer to the $T=0$ ($T=1$) dominant states as the $T=0$ ($T=1$) states throughout this paper. The spatial amplitudes $\phi_I^{(c)}$ are expanded in terms of the Gaussian basis functions in the same way as Eq. (2.4) and Eq. (2.5). The angular-momentum space and the optimized Gaussian range parameters employed for the $J=0^+$ states of ^{6}He, ^{6}Li ($T=1$), and ^{6}Be are listed in Table III as an example. The results of the calculation will be discussed together with those of $A=7$ hypernuclei.

B. The model for $A=7$ hypernuclei

By employing the ${}^{5}_{\Lambda}$He$+N+N$ model for $A=7$ hypernuclei, the total Hamiltonian is written as

$$H=T+V_{{}^{5}_{\Lambda}\text{He-}N_1}(\mathbf{r}_1)+V_{{}^{5}_{\Lambda}\text{He-}N_2}(\mathbf{r}_2)+V_{N_1N_2}(\mathbf{r}_3)+V_{\text{Pauli}}. \tag{3.3}$$

For the NN interaction $V_{N_1N_2}$, we employ the same Bonn A potential as used in the $A=6$ nuclei. $V_{{}^{5}_{\Lambda}\text{He}-N}$ is the interaction between the ${}^{5}_{\Lambda}$He cluster and a valence nucleon. The total wave function is expressed by

$$\Psi_{JM}({}^{7}_{\Lambda}Z)=\sum_{c=1}^{3}\sum_{I,S}[\Phi_{1/2}({}^{5}_{\Lambda}\text{He})[\phi_I^{(c)}(\mathbf{r}_c,\mathbf{R}_c) \times[\chi_{1/2}(N_1)\chi_{1/2}(N_2)]_S]_{J_0}]_{JM}. \tag{3.4}$$

Here $\Phi_{1/2}({}^{5}_{\Lambda}\text{He})$ denotes the wave function of ${}^{5}_{\Lambda}$He with spin 1/2 which couples with J_0 to the total angular-momentum $J=J_0\pm 1/2$. The spatial amplitudes $\Phi_I^{(c)}$ are expanded in terms of the Gaussian basis functions in the same way as Eq. (2.4) and Eq. (2.5). The angular-momentum space and the Gaussian range parameters employed for the $1/2^+$ states of

$^{7}_{\Lambda}$He, $^{7}_{\Lambda}$Li ($T=1$), and $^{7}_{\Lambda}$Be are the same as those in Table III for the $A=6$ nuclei ($T=1$).

As for the interaction between the valence nucleon and the $^{5}_{\Lambda}$He core, $V_{^{5}_{\Lambda}\text{He-}N}$, we employed the following approximation. In order to take the Pauli operator V_{Pauli} into account exactly within the $^{5}_{\Lambda}\text{He}+N+N$ model, the center of mass of $^{5}_{\Lambda}$He is assumed to be located at that of the α particle. The interaction $V_{^{5}_{\Lambda}\text{He-}N}$ is composed of the sum of the αN part, $V_{\alpha N}$, and the ΛN part, which is given by folding $V_{\Lambda N}$ into the density of Λ in $^{5}_{\Lambda}$He.

In addition, we slightly modify the interaction so that the $^{5}_{\Lambda}\text{He}+N$ model can reproduce the observed ground-state energy of $^{6}_{\Lambda}$He ($^{6}_{\Lambda}$Li) and the 1^{-} - 2^{-} splitting given by the full $\alpha+\Lambda+N$ model (the 2^{-} is not observed yet); we thus tuned $V_{^{5}_{\Lambda}\text{He-}N}$ by changing η from 0.1 to 0.2 and multiplying the total strength of $V_{^{5}_{\Lambda}\text{He-}N}$ by a factor of 0.98.

C. Results and discussion

The calculated energy spectra of the low-lying states of $^{7}_{\Lambda}$He, $^{7}_{\Lambda}$Li ($T=1$), and $^{7}_{\Lambda}$Be are illustrated in Fig. 4 in comparison with the calculated spectra of the corresponding $A=6$ nuclei. The energy positions of resonant states are determined by examining their stabilization with respect to extension of the basis space. The resonant states are well distinguished from discretized nonresonant continuum states by checking the wave function distribution over the internal and external regions. It is naturally seen in Fig. 4 that, as the proton number increases, the low-lying states in the $A=7$ hypernuclei go upward in parallel with the $A=6$ nuclei.

The energy values are summarized in Table IV together with the rms distances $\overline{r^{2}_{^{5}_{\Lambda}\text{He-}N}}$, $\overline{r^{2}_{N_1\text{-}N_2}}$, and $\overline{r^{2}_{^{5}_{\Lambda}\text{He-}N_1N_2}}$ which are defined in the same manner as in Eqs. (2.7) and (2.8). For example,

$$\overline{r^{2}_{^{5}_{\Lambda}\text{He-}N_1}}=\left[4\pi\int r_1^2\rho_{N_1}(r_1)r_1^2dr_1\right]^{1/2}, \tag{3.5}$$

where $\rho_{N_1}(r_1)$ is the nucleon density as a function of the $^{5}_{\Lambda}\text{He-}N_1$ distance r_1:

$$\rho_N(r_1)=\int |\Psi_{JM}(^{7}_{\Lambda}Z)|^2 d\mathbf{R}_1 d\hat{\mathbf{r}}_1/4\pi. \tag{3.6}$$

The theoretical Λ binding energy (B_Λ = 5.00 MeV) of $^{7}_{\Lambda}$Be agrees satisfactorily with the observed value (5.16 MeV). The hypernucleus $^{7}_{\Lambda}$Be, which is regarded as a weakly coupled $^{5}_{\Lambda}\text{He}+p+p$ system, is an interesting three-body system from the viewpoint that it is totally bound but none of the two-body subsystems are bound. This type of three-body system is called a Borromean [11], and there are several examples in nuclei such as ^{6}He $=\alpha+n+n$, ^{9}Be $=2\alpha+n$, ^{11}Li = ^{9}Li + $2n$, and ^{12}C = 3α in which we see always $N\geqslant Z$ for the neutron and proton numbers. But the case of $^{7}_{\Lambda}$Be is $N<Z$; namely, to the authors' knowledge, it is considered to be the only case of a *proton-rich* Borromean so far reported in nuclei and hypernuclei. We found that, theoretically, the binding of this $^{5}_{\Lambda}\text{He}+p+p$ system is reproduced by taking fully into account the p-p correlation with a realistic NN interaction and by adopting the basis functions of all three rearrangement channels.

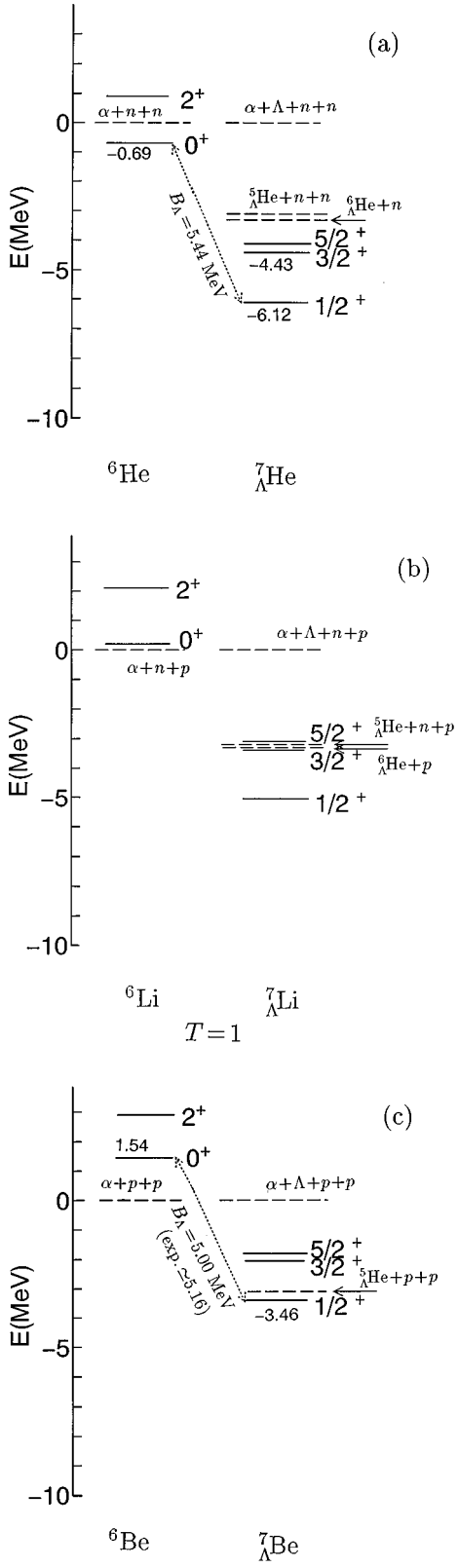

FIG. 4. Calculated energy spectra of the low-lying states of (a) $^{7}_{\Lambda}$He, (b) $^{7}_{\Lambda}$Li ($T=1$), and, (c) $^{7}_{\Lambda}$Be together with those of the corresponding nuclei ^{6}He, ^{6}Li ($T=1$), and ^{6}Be.

The agreement of the calculated binding energy of $^{7}_{\Lambda}$Be with the observed one gives support to the present $^{5}_{\Lambda}\text{He}+$

TABLE IV. Calculated energies of the low-lying states of (a) ${}^{7}_{\Lambda}$He, (b) ${}^{7}_{\Lambda}$Li ($T=1$), and (c) ${}^{7}_{\Lambda}$Be together with those of the corresponding nuclei ^{6}He, ^{6}Li ($T=1$), and ^{6}Be, respectively. The energies E are measured from the $\alpha+N+N$ threshold for the $A=6$ nuclei and from the $\alpha+\Lambda+N+N$ threshold for $A=7$ hypernuclei. The energies in parentheses are measured from the ${}^{6}_{\Lambda}$He $+N$ threshold for ${}^{7}_{\Lambda}$He and ${}^{7}_{\Lambda}$Li ($T=1$) and from ${}^{5}_{\Lambda}$He$+p+p$ for ${}^{7}_{\Lambda}$Be. The rms distances $\overline{r_{\text{core-}N}}$, $\overline{r_{N_1\text{-}N_2}}$, and $\overline{r_{\text{core-}N_1N_2}}$ are also given for bound states. Here, ''core'' denotes α or ${}^{5}_{\Lambda}$He.

(a)

	^{6}He		${}^{7}_{\Lambda}$He		
J	0^+	2^+	$1/2^+$	$3/2^+$	$5/2^+$
E (MeV)	−0.70	0.88	−6.12	−4.43	−4.08
			(−2.83)	(−1.14)	(−0.78)
E^{expt} (MeV)	−0.98	0.83			
B_Λ (MeV)			5.44		
B_Λ^{expt} (MeV)					
$\overline{r_{\text{core-}n}}$ (fm)	4.55		3.55	3.93	4.05
$\overline{r_{\text{core-}2n}}$ (fm)	3.79		2.90	3.01	3.11
$\overline{r_{n\text{-}n}}$ (fm)	4.68		4.11	5.06	5.17

(b)

	^{6}Li ($T=1$)		${}^{7}_{\Lambda}$Li ($T=1$)		
J	0^+	2^+	$1/2^+$	$3/2^+$	$5/2^+$
E (MeV)	0.20	2.11	−5.05	−3.42	−3.09
			(−1.76)	(−0.13)	(0.20)
E^{expt} (MeV)	−0.14	1.67			
B_Λ (MeV)			1.59		
B_Λ^{expt} (MeV)					
$\overline{r_{\text{core-}n}}$ (fm)			3.62	4.05	
$\overline{r_{\text{core-}p}}$ (fm)			3.74	4.57	
$\overline{r_{\text{core-}p}}$ (fm)			3.01	3.29	
$\overline{r_{n\text{-}p}}$ (fm)			4.23	5.59	

(c)

	^{6}Be		${}^{7}_{\Lambda}$Be		
J	0^+	2^+	$1/2^+$	$3/2^+$	$5/2^+$
E (MeV)	1.54	2.93	−3.46	−2.05	−1.77
			(−0.34)	(1.07)	(1.25)
E^{expt} (MeV)	1.37	3.04	−3.79		
			(−0.67)		
B_Λ (MeV)			5.00		
B_Λ^{expt} (MeV)			5.16		
$\overline{r_{\text{core-}p}}$ (fm)			3.95		
$\overline{r_{\text{core-}2p}}$ (fm)			3.23		
$\overline{r_{p\text{-}p}}$ (fm)			4.55		

$N+N$ model for the $A=7$ hypernuclei. There are no experimental data for ${}^{7}_{\Lambda}$He and ${}^{7}_{\Lambda}$Li ($T=1$). We predict the Λ binding energies of those hypernuclei to be 5.44 MeV and 1.59 MeV, respectively. The values will not change significantly even if any other ΛN interaction is adopted, as long as the calculation satisfies the condition that the observed binding energy of ${}^{7}_{\Lambda}$Be is reproduced with that interaction. Observation of γ transitions among the $1/2^+$, $3/2^+$, and $5/2^+$ states in ${}^{7}_{\Lambda}$He would be very useful to further discussion on the structure of this hypernucleus [26]. This information would also be helpful to the study of the excitation mechanism of the halo nucleus ^{6}He since the γ transition cannot be observed in the nucleus due to the prompt particle decay of the corresponding excited state (2^+).

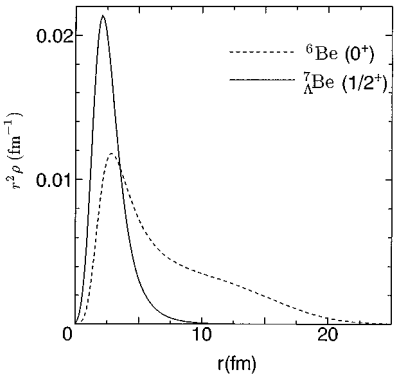

FIG. 5. Density distributions of the valence proton, ρ_p, in the ground states of ^{6}Be and ${}^{7}_{\Lambda}$Be, multiplied by r^2. The radius r is measured from the c.m. of the core.

It is particularly interesting to see the gluelike role of the Λ particle in $T=1$ hypernuclear systems. Though the ground state of ^{6}Be is unbound, the Λ participation leads to a weakly bound ground state of ${}^{7}_{\Lambda}$Be. Figure 5 demonstrates the strong shrinkage of the valence-proton density in ${}^{7}_{\Lambda}$Be from that in ^{6}Be (the density of this resonant state is normalized to unity within 25 fm). The ground state of the nucleus ^{6}He is only weakly bound by 0.69 MeV below the $\alpha+2n$ threshold in the present calculation, while that of ${}^{7}_{\Lambda}$He becomes rather deeply bound by 3.02 MeV below the ${}^{5}_{\Lambda}$He $+2n$ threshold. Similar behavior is seen for the lowest-lying $T=1$ state of ^{6}Li and ${}^{7}_{\Lambda}$Li. In general, the two-nucleon separation energy becomes larger by 1.6–2.1 MeV due to the presence of the Λ particle in these $T=1$ hypernuclear states.

The present calculation predicts very weakly bound states with respect to the ${}^{6}_{\Lambda}$He $+N$ thresholds: $5/2^+$ in ${}^{7}_{\Lambda}$He, $3/2^+$ in ${}^{7}_{\Lambda}$Li, and $1/2^+$ state in ${}^{7}_{\Lambda}$Be. It is thus interesting to examine whether or not these states exhibit any halo structure having a long tail of the density distribution of the valence nucleon. Let us start with ${}^{7}_{\Lambda}$He ($5/2^+$) listed in Table IV(a). The two-neutron separation energy of this state is 0.79 MeV, which is close to the two-neutron separation energy (0.975 MeV) of the halo nucleus ^{6}He. Nevertheless, the neutron rms distance $\overline{r_{{}^{5}_{\Lambda}\text{He-}n}} = 4.05$ fm is not as large as $\overline{r_{\alpha\text{-}n}} = 4.55$ fm of ^{6}He. This is due to the role of the centrifugal barrier ($L=2$) between the c.m. of two neutrons and ${}^{5}_{\Lambda}$He in the $5/2^+$ state, while the ^{6}He halo bound state has the $L=0$ component predominantly.

As seen in Table IV(b), in the $T=1$, $3/2^+$ state in ${}^{7}_{\Lambda}$Li, the calculated rms distance of the valence proton from the core, $\overline{r_{{}^{5}_{\Lambda}\text{He-}p}} = 4.57$ fm, is almost the same as $\overline{r_{\alpha\text{-}n}}$ in the halo nucleus ^{6}He. Therefore we consider that this state has the possibility of a halo structure. On the other hand, the neutron distance in the state is shorter by 0.5 fm than the proton one. This is because the ${}^{5}_{\Lambda}$He$+n$ subsystem has a bound state, while the ${}^{5}_{\Lambda}$He $+p$ subsystem does not. Therefore the valence neutron is located closer to the ${}^{5}_{\Lambda}$He core than the proton is. As for the $1/2^+$ state in ${}^{7}_{\Lambda}$Be [Table IV(c)],

$r\ \overline{{}^{5}_{\Lambda}\text{He-}p} = 3.9$ fm is shorter by 0.5 fm than $\overline{r^{5}_{\Lambda}\text{He-}p}$ in the $3/2^+$ state in ${}^{7}_{\Lambda}$Li. Therefore the proton tail of ${}^{7}_{\Lambda}$Be is not considered to be halolike. Though the state is only 0.3 MeV bound below the three-body breakup threshold, the fact that $r\ \overline{{}^{5}_{\Lambda}\text{He-}p}$ is not very large is attributed to the Coulomb barrier between the ${}^{5}_{\Lambda}$He cluster and the two valence protons.

In the above discussion we have compared the calculated results from the viewpoint of the rms distance of the valence nucleon from the core. In order to confirm the above discussions, we illustrate the density distributions $\rho_N(r)$ of the valence nucleon in Figs. 6(a), 6(b) and 6(c), respectively. For definition of $\rho_N(r)$, see Eq. (3.6). We see that the proton density in the $3/2^+$ state in ${}^{7}_{\Lambda}$Li is the most extended to the long-range region, when compared among the three cases concerned here. It is interesting that the extended distribution of $\rho_p(r)$ for ${}^{7}_{\Lambda}$Li $(3/2^+)$ is comparable to the neutron halo density $\rho_n(r)$ for ^{6}He (0^+). Note, however, that the density extension for the remaining two cases for ${}^{7}_{\Lambda}$He $(5/2^+)$ and ${}^{7}_{\Lambda}$Be $(1/2^+)$ is not so pronounced, but rather skinlike.

IV. $T=0$ STATES OF ${}^{7}_{\Lambda}$Li

A. A limitation of the $\alpha+d+\Lambda$ model

In order to get information on the spin-spin term of the ΛN interaction, it is particularly useful to calculate the splittings of the Λ spin-doublet states of ${}^{7}_{\Lambda}$Li. Using a microscopic $\alpha+d+\Lambda$ model, the spin-doublet splittings have been investigated in Refs. [1,20,24], where the effective ΛN interactions are folded into the nucleon density of ^{6}Li constructed on the basis of the OCM for the $\alpha+d$ clusters. In general, before doing three-body calculations, it is desirable that observed binding energies of all the two-body subsystems are reproduced by the employed interactions. In view of this, the previous $\alpha+d+\Lambda$ models [1,20,24] are not always satisfactory, since the ΛN effective interactions adopted to explain the binding energy of the $\alpha+\Lambda$ subsystem lead inevitably to an underestimate for the $d+\Lambda$ part.

Here, let us perform a trial calculation by multiplying the $d\Lambda$ interaction part by a factor of 1.20 so as to reproduce $B_\Lambda({}^{3}_{\Lambda}\text{H})$. We then find that this change of the $d\Lambda$ interaction leads to $B_\Lambda({}^{7}_{\Lambda}\text{Li}) = 7.10$ MeV, resulting in overbinding by 1.5 MeV with respect to the observed value (5.58 MeV), and that a larger value (1.5 MeV) is obtained for the $3/2^+$-$1/2^+$ splitting in comparison with the previous estimates (1.1 and 1.3 MeV) [1,20]. This overbinding of ${}^{7}_{\Lambda}$Li derived from the $\alpha+d+\Lambda$ model suggests that the deuteron cluster in ${}^{7}_{\Lambda}$Li is very different from that in ${}^{3}_{\Lambda}$H [25], the latter being quite similar to the isolated deuteron. Thus, in order to extract a reliable spectroscopic information on the ΛN spin-spin interaction, it is necessary to take fully into account the degree of freedom of the n-p relative motion without assuming a frozen deuteron cluster in ${}^{7}_{\Lambda}$Li.

Therefore it is desirable at best to investigate ${}^{7}_{\Lambda}$Li with the four-body $\alpha+\Lambda+n+p$ model. As far as the framework of three-body models is concerned, however, the ${}^{5}_{\Lambda}\text{He}+n+p$ model adopted in the previous section should be more suited to describe the $T=0$ ${}^{7}_{\Lambda}$Li states than the $\alpha+d+\Lambda$ model. Using the ${}^{5}_{\Lambda}\text{He}+n+p$ model, we shall discuss the probability for the valence neutron and proton to compose a deuteron cluster.

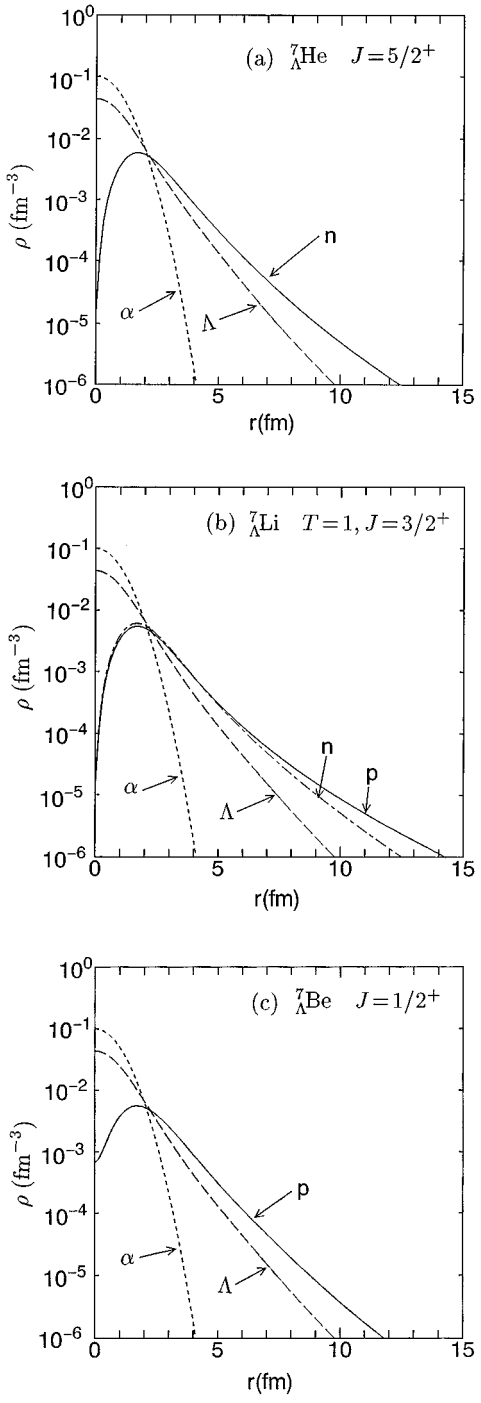

FIG. 6. Density distributions of the valence nucleon in the very weakly bound states of (a) ${}^{7}_{\Lambda}$He $(5/2^+)$, (b) ${}^{7}_{\Lambda}$Li $(T=1, 3/2^+)$, and (c) ${}^{7}_{\Lambda}$Be $(1/2^+)$. Those of the Λ particle and a single nucleon in the ${}^{5}_{\Lambda}$He cluster are compared in each block. The radius r is measured from the c.m. of ${}^{5}_{\Lambda}$He.

B. Results with the ${}^{5}_{\Lambda}\text{He}+n+p$ model

With the use of the $\alpha+n+p$ and ${}^{5}_{\Lambda}\text{He}+n+p$ models described in Sec. III (cf. Fig. 3), calculations were made for the low-lying $T=0$ states of ^{6}Li and ${}^{7}_{\Lambda}$Li, respectively. The adopted angular-momentum space and the optimized Gauss-

TABLE V. The angular-momentum model space of the three-body basis functions (3.4) and the Gaussian range parameters (2.5) employed for the ground state of ${}^{7}_{\Lambda}$Li ($T=0$). Also see comments for Table I.

c	l	L	I	S	J_0	$n_{\max}$	$r_{\min}$	$r_{\max}$	$N_{\max}$	$R_{\min}$	$R_{\max}$
c_1	1	1	0	1	1	8	0.5	7.0	8	0.5	8.0
c_1	1	1	1	0	1	8	0.5	7.0	8	0.5	8.0
c_1	1	1	1	1	1	8	0.5	7.0	8	0.5	8.0
c_2	1	1	0	1	1	8	0.5	7.0	8	0.5	8.0
c_2	1	1	1	0	1	8	0.5	7.0	8	0.5	8.0
c_2	1	1	1	1	1	8	0.5	7.0	8	0.5	8.0
c_3	0	0	0	1	1	10	0.1	7.0	10	0.5	8.0
c_3	2	0	2	1	1	10	0.2	7.0	10	0.5	8.0
c_3	0	2	2	1	1	8	0.1	7.0	8	0.5	8.0
c_3	2	2	2	1	1	8	0.2	7.0	8	0.5	8.0
c_3	2	2	1	1	1	8	0.2	7.0	8	0.5	8.0
c_3	2	2	0	1	1	8	0.2	7.0	8	0.5	8.0

ian range parameters of the basis functions [cf. Eqs. (2.4), (2.5), and (3.4)] are listed in Table V for the ground state of ${}^{7}_{\Lambda}$Li. The calculated energy spectra are illustrated in Fig. 7. The energies and the rms distances are summarized in Table VI. The energies are well converged on increasing the number of basis functions. As is known, it is difficult, within the bound-state approximation method, to predict a stable and reliable value of the energy of *broad* resonances. Therefore we do not report here the energies of the resonant $T=0$, 2^+, and 1^+_2 states of ^{6}Li and the corresponding states of ${}^{7}_{\Lambda}$Li. We shall investigate those states on the basis of the complex-coordinate rotation method [27] for resonant states when we apply the $\alpha+\Lambda+n+p$ model to the $A=7$ Λ hypernuclei in the near future.

It is interesting to note that the observed Λ binding energy of ${}^{7}_{\Lambda}$Li is satisfactorily reproduced by the ${}^{5}_{\Lambda}$He$+n+p$

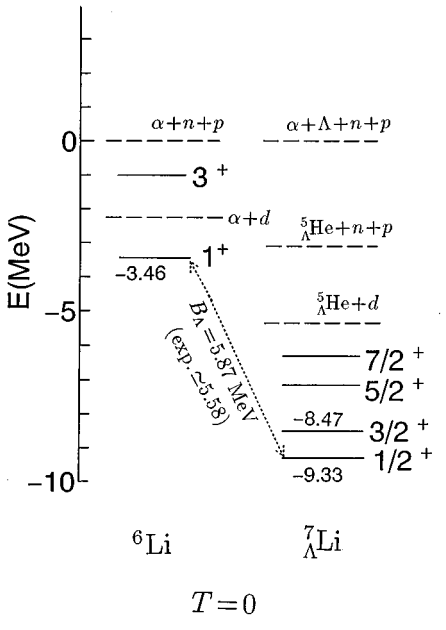

FIG. 7. Calculated energy spectra of the low-lying states of ${}^{7}_{\Lambda}$Li ($T=0$) with those of the corresponding nucleus ^{6}Li ($T=0$).

TABLE VI. Calculated energies of the low-lying states of ${}^{7}_{\Lambda}$Li ($T=0$) together with those of the corresponding nucleus ^{6}Li ($T=0$). The energies E are measured from the $\alpha+n+p$ breakup threshold for ^{6}Li and from the $\alpha+\Lambda+n+p$ threshold for ${}^{7}_{\Lambda}$Li. The energies in parentheses are measured from the $\alpha+d$ threshold for ^{6}Li and the ${}^{5}_{\Lambda}$He $+$ d threshold for ${}^{7}_{\Lambda}$Li. The rms distances $\overline{r}_{\text{core-}n}$, $\overline{r}_{\text{core-}p}$, $\overline{r}_{\text{core-}np}$, and $\overline{r}_{n\text{-}p}$ are also shown for bound states. Here, ''core'' denotes α or ${}^{5}_{\Lambda}$He.

	^{6}Li ($T=0$)		${}^{7}_{\Lambda}$Li ($T=0$)			
J	1^+	3^+	$1/2^+$	$3/2^+$	$5/2^+$	$7/2^+$
E (MeV)	−3.46	−0.99	−9.33	−8.47	−7.14	−6.33
	(−1.24)	(1.23)	(−3.99)	(− 3.13)	(−1.80)	(−0.99)
E^{expt} (MeV)	−3.70	−1.51	−9.28		− 7.25	
	(−1.48)	(0.71)	(−3.94)		(−1.91)	
B_Λ (MeV)			5.87			
B_Λ^{expt} (MeV)			5.58			
$\overline{r}_{\text{core-}n}$ (fm)	4.19		3.36	3.50	3.30	3.45
$\overline{r}_{\text{core-}p}$ (fm)	4.23		3.39	3.53	3.35	3.51
$\overline{r}_{\text{core-}np}$ (fm)	3.85		2.94	3.08	2.78	2.93
$\overline{r}_{n\text{-}p}$ (fm)	3.42		3.33	3.38	3.67	3.76

calculation: The difficulty of overbinding encountered in the $\alpha+d+\Lambda$ model is not seen here. This is due to the fact that deuteron excitation is allowed in the present model. This also results in the slight reduction of the ground-state doublet splitting to 0.9 MeV from the values 1.1–1.5 MeV obtained by the $\alpha+d+\Lambda$ model. The excitation energy of the $5/2^+$ state, 2.19 MeV, corresponds well to the observed γ transition energy of 2.03 MeV. The $7/2^+$ state is weakly bound with respect to the ${}^{5}_{\Lambda}$He $+$ d threshold, but the centrifugal barrier ($L=2$) between ${}^{5}_{\Lambda}$He and the n-p pair prevents the state from having a halolike long-range tail.

In order to investigate the behavior of the valence n-p pair in the ground state of ${}^{7}_{\Lambda}$Li, we introduce two types of probabilities and compare them. The first one is the probability density, $\rho_{n\text{-}p}(R_3)$, which is defined as the probability to find the c.m. of the n-p pair at a distance R_3 from ${}^{5}_{\Lambda}$He [cf. Fig. 3 ($c=3$)]:

$$\rho_{n\text{-}p}(R_3)=\int |\Psi({}^{7}_{\Lambda}\text{Li,g.s.})|^2 d\mathbf{r}_3 d\hat{\mathbf{R}}_3/4\pi. \tag{4.1}$$

This probability density has the normalization

$$4\pi\int \rho_{n\text{-}p}(R_3)R_3^2 dR_3=1. \tag{4.2}$$

The second one is the probability density $\rho_d(R_3)$ that the n-p pair is found as a deuteron cluster at a distance R_3:

$$\rho_d(R_3)=\sum_m \int \left| \int \phi^*_{1^+m}(\mathbf{r}_3)\Psi({}^{7}_{\Lambda}\text{Li,g.s.})d\mathbf{r}_3 \right|^2 d\hat{\mathbf{R}}_3/4\pi, \tag{4.3}$$

where $\phi^*_{1^+m}$ is the deuteron wave function calculated with the same $V_{N_1N_2}$ of Eq. (3.3). The integrated probability of deuteron clusterization P_d is defined by

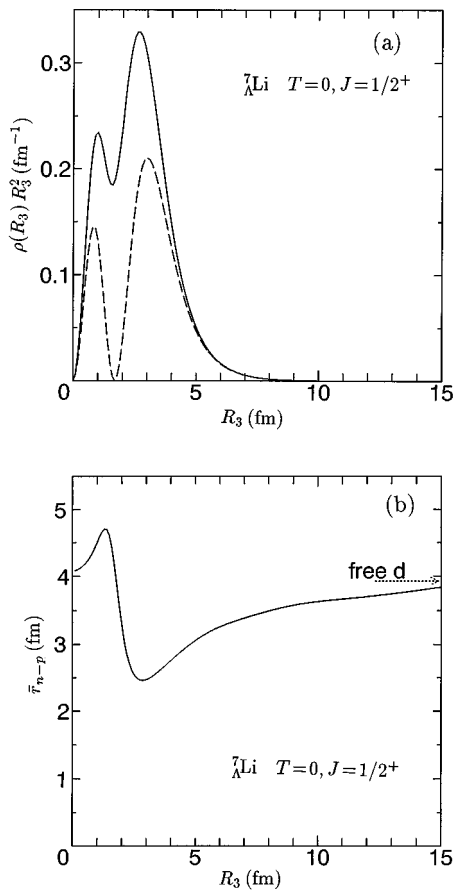

FIG. 8. (a) Probability density $\rho(R_3)$ of finding the valence n-p pair in the ground state of $^{7}_{\Lambda}$Li drawn as a function of the distance R_3 between the c.m. of the pair and $^{5}_{\Lambda}$He (solid line). The dashed line shows the probability density of finding the deuteron, $\rho(R_3)$; see Eqs. (4.1) and (4.3) for definition. (b) The internal distance of the valence n-p pair in the ground state of $^{7}_{\Lambda}$Li as a function of R_3. The n-p distance of the free deuteron (3.9 fm) is indicated by an arrow.

$$P_d = \int \rho_d(R_3) R_3^2 dR_3 . \tag{4.4}$$

Furthermore, in order to see explicitly how the internal distance between n-p pairs changes as the c.m. of the pair approaches the $^{5}_{\Lambda}$He core, we introduce an averaged distance between n and p, $\overline{r_{n\text{-}p}}(R_3)$, at a particular distance R_3:

$$\overline{r_{n\text{-}p}}(R_3) = \left[\int |\Psi(^{7}_{\Lambda}\mathrm{Li,g.s.})|^2 r_3^2 d\mathbf{r}_3 d\hat{\mathbf{R}}_3 / 4\pi \rho_{n\text{-}p}(R_3) \right]^{1/2} . \tag{4.5}$$

The calculated densities $\rho_{n\text{-}p}(R_3)$ and $\rho_d(R_3)$ multiplied by R_3^2 are illustrated in Fig. 8(a) together with $\overline{r_{n\text{-}p}}(R_3)$ in Fig. 8(b). It is noted first that the node of $\rho_d(R_3)$ seen at $R_3 = 1.7$ fm comes from the Pauli principle that the relative motion between the deuteron cluster and $^{5}_{\Lambda}$He should be orthogonal to the lowest $0S$ state. However, such a nodal behavior is much reduced in $\rho_{n\text{-}p}(R_3)$ because even the $0S$ component is allowed when the deuteron is excited internally. As is expected, in the region far from the surface, the probability of deuteron clusterization is large ($\rho_d/\rho_{n\text{-}p} \simeq 1$) and the internal distance $\overline{r_{n\text{-}p}}(R_3)$ is close to the size of the free deuteron. On the other hand, as the n-p pair approaches the $^{5}_{\Lambda}$He core, the ratio $\rho_d/\rho_{n\text{-}p}$ decreases drastically. At $R_3 \simeq 3$ fm, the n-p pair density $\rho_{n\text{-}p}(R_3)$ is largest, but the deuteron is broken by about 40% ($\rho_d/\rho_{n\text{-}p} \simeq 0.6$) and the n-p internal size $\overline{r_{n\text{-}p}}(R_3)$ takes the smallest value of 2.4 fm, which is sizably reduced from the free deuteron size (3.94 fm). As a result, the integrated probability of deuteron clusterization is as small as $P_d = 0.57$. In the case of the ^{6}Li nucleus, similar behavior of $\rho_{n\text{-}p}$ and ρ_d is seen, but the peak position is slightly displaced toward the outside, resulting in a larger value of $P_d = 0.65$. The gluelike effect of the Λ particle in $^{7}_{\Lambda}$Li works to break the deuteron cluster more than in ^{6}Li.

When $^{7}_{\Lambda}$Li is excited so as to have $J = 5/2^{+}$, the distance between $^{5}_{\Lambda}$He and the n-p pair contracts slightly (Table VI) due to the angular-momentum barrier ($L = 2$) between them. This is the same result as obtained in the $\alpha + d + \Lambda$ model calculations [1,20]. On the other hand, it should be emphasized here that the internal distance of the n-p pair increases appreciably (Table VI). This causes an enhancement of the deuteron clusterization from $P_d(1/2^{+}) = 0.57$ to $P_d(5/2^{+}) = 0.61$, though the c.m. of the n-p pair is closer to the core in the excited state.

From the above demonstration we conclude that, when one discusses the details of the energy level structure of $^{7}_{\Lambda}$Li in close connection with the ΛN interaction properties, the freedom of the n-p relative motion should be fully taken into account.

V. SUMMARY

We have studied dynamical features predicted within the extended three-body model for the hypernuclei with $A = 6$ ($^{6}_{\Lambda}$He and $^{6}_{\Lambda}$Li) and $A = 7$ ($^{7}_{\Lambda}$He, $^{7}_{\Lambda}$Li, and $^{7}_{\Lambda}$Be). Most of the states studied in this paper are located near the $\alpha + \Lambda + N$ and $^{5}_{\Lambda}\mathrm{He} + N + N$ thresholds, respectively. On the basis of careful calculations, we have proven that the picture of $^{5}_{\Lambda}$He plus two valence nucleons works quite well in describing the $A = 7$ hypernuclei.

In order to describe these types of states properly, we took the coupled-rearrangement-channel variational method with the use of Jacobian-coordinate Gaussian basis functions [6–8]. As for the ΛN interaction, use was made of an effective interaction with one-range Gaussian (ORG) shape which has often been adopted in the calculations of light hypernuclei. We employed the appropriate αN interaction which reproduces the low-energy αN scattering data very well. The major results obtained for $^{6}_{\Lambda}$He, $^{6}_{\Lambda}$Li, $^{7}_{\Lambda}$He, $^{7}_{\Lambda}$Li, and $^{7}_{\Lambda}$Be are summarized as follows.

(1) The observed ground-state energies of $^{6}_{\Lambda}$He and $^{6}_{\Lambda}$Li are satisfactorily reproduced by the $\alpha + \Lambda + N$ model with coupled rearrangement channels. $^{6}_{\Lambda}$He is found to have a three-layer structure of matter distribution: the α core, the Λ skin, and the neutron halo. It is notable that the $^{5}_{\Lambda}$He hypernucleus behaves as a good core cluster in $^{6}_{\Lambda}$He and $^{6}_{\Lambda}$Li.

(2) The $\alpha + p + p$ and $^{5}_{\Lambda}\mathrm{He} + p + p$ models reproduce the observed energies of the resonant ground state of the ^{6}Be

nucleus and the loosely bound ground state of the ${}^{7}_{\Lambda}$Be hypernucleus, respectively. The p-p correlation in the presence of the Λ particle makes ${}^{7}_{\Lambda}\mathrm{Be}={}^{5}_{\Lambda}\mathrm{He}+p+p$ bound; this might be the only *proton-rich* Borromean system. The valence protons in ${}^{7}_{\Lambda}$Be show not a halolike but a skinlike density distribution due to suppression of the tail region by the Coulomb potential barrier.

(3) We predict that the addition of a Λ particle to the typical neutron halo nucleus ^{6}He results in the stabilized $1/2^{+}$ ground state of ${}^{7}_{\Lambda}$He at 2.83 MeV below the ${}^{6}_{\Lambda}\mathrm{He}+n$ threshold [$B_{\Lambda}({}^{7}_{\Lambda}\mathrm{He})=5.44$ MeV]. This prediction will hold for any other ΛN interaction as long as the calculation satisfies the condition that the observed binding energy of ${}^{7}_{\Lambda}$Be is reproduced with that interaction. The excited spin-doublet states with $J=5/2^{+}$ and $3/2^{+}$ become weakly bound. The neutron distribution is skinlike, similar to that of ${}^{7}_{\Lambda}$Be. Observation of γ transitions among the $1/2^{+}$, $3/2^{+}$, and $5/2^{+}$ states would be very useful to further discussion on the structure of ${}^{7}_{\Lambda}$He.

(4) The addition of a Λ particle to the $T=1,2^{+}$ state ($E_x=5.38$ MeV) of ^{6}Li generates a proton halo $3/2^{+}$ state in ${}^{7}_{\Lambda}$Li. Due to the presence of the Λ particle, in general, the $A=7$ hypernuclei are stabilized by 1.6–2.1 MeV compared with the $A=6$ core nuclei.

(5) In the $T=0$ states of ${}^{7}_{\Lambda}$Li, the probability of deuteron clustering is found to be only 57%. Instead of the $\alpha+d+\Lambda$ model, we took the ${}^{5}_{\Lambda}\mathrm{He}+n+p$ model with full account of the n-p correlation. The model reproduces the binding energy of the ground state of ${}^{7}_{\Lambda}$Li, and reduces appreciably the splitting of the Λ spin doublets in comparison with the frozen-deuteron approximation.

The ${}^{7}_{\Lambda}$Li hypernucleus is an important system to obtain information on the spin-spin term of the ΛN interaction through the spin-doublet states. In this respect an extended calculation with a four-body $\alpha+\Lambda+n+p$ model may be necessary to confirm the predictions by the ${}^{5}_{\Lambda}\mathrm{He}+n+p$ model. Also, use of more realistic effective interactions in place of ORG is particularly desirable, not only for the study of the $T=0$ low-lying states of ${}^{7}_{\Lambda}$Li, but also for more extended investigation of the loosely coupling states in the ${}^{7}_{\Lambda}$He, ${}^{7}_{\Lambda}$Li ($T=1$), and ${}^{7}_{\Lambda}$Be hypernuclei. Such a four-body $\alpha+\Lambda+N+N$ model calculation is in progress.

ACKNOWLEDGMENTS

The authors would like to thank Professor K. Ikeda for helpful discussions and encouragement. This work has been supported in part by the Japan Society for the Promotion of Science (E.H.) and a Grant-in-Aid for Scientific Research.

[1] T. Motoba, H. Bandō, and K. Ikeda, Prog. Theor. Phys. **70**, 189 (1983); T. Motoba, H. Bandō, K. Ikeda, and T. Yamada, Prog. Theor. Phys. Suppl. No. 81, 42 (1985).
[2] H. Bandō, T. Motoba, and J. Žofka, Int. J. Mod. Phys. A **5**, 4021 (1990).
[3] For recent topics, see Physics of Unstable Nuclei, Proceedings of the 5th International Symposium, Niigata, 1994, edited by H. Horiuchi, K. Ikeda, K. Sato, Y. Suzuki, and I. Tanihata [Nucl. Phys. **A588** (1) (1995)].
[4] L. Majling, in *Few-Body Problems in Physics, Proceedings of the National Conference on Physics of Few-Body and Quark-Hadronic Systems*, Kharkov, Ukraine, 1992, edited by V. Boldyshev, V. Kotlyar, and A. Shebeko (KFTI, Kharkov, 1994), p. 345.
[5] A. Gal, Adv. Nucl. Phys. **8**, 1 (1975).
[6] M. Kamimura, Phys. Rev. A **38**, 621 (1988).
[7] H. Kameyama, M. Kamimura, and Y. Fukushima, Phys. Rev. C **40**, 974 (1989).
[8] E. Hiyama and M. Kamimura, Nucl. Phys. **A588**, 35c (1995).
[9] M. Jurič *et al.*, Nucl. Phys. **B52**, 1 (1973).
[10] R. Bertini *et al.*, Nucl. Phys. **A368**, 365 (1981).
[11] M.V. Zhukov, B.V. Danilin, D.V. Fedorov, J.M. Bang, I.J. Thompson, and J.S. Vaagen, Phys. Rep. **231**, 151 (1994).
[12] R. Machleidt, Adv. Nucl. Phys. **19**, 189 (1989).
[13] I. Tanihata *et al.*, Phys. Lett. **160B**, 380 (1985).
[14] Y. Suzuki, Nucl. Phys. **A528**, 395 (1991).
[15] S. Funada, H. Kameyama, and Y. Sakuragi, Nucl. Phys. **A575**, 93 (1994).
[16] V.I. Kukulin, V.N. Pomerantsev, Kh.D. Razikov, V.T. Voronchev, and G.G. Ryzhikh, Nucl. Phys. **A586**, 151 (1995).
[17] O. Richter, M. Sotona, and J. Žofka, Phys. Rev. C **43**, 2753 (1991).
[18] V.N. Fetisov, L. Majling, J. Žofka, and R.A. Eramzhyan, Z. Phys. A **339**, 399 (1991).
[19] K. Arai, Y. Suzuki, and K. Varga, Phys. Rev. C **51**, 2488 (1995).
[20] Wang Xi-cang, H. Bandō, and H. Takaki, Z. Phys. A **327**, 59 (1987).
[21] S. Saito, Prog. Theor. Phys. **41**, 705 (1969).
[22] V.I. Kukulin, V.M. Krasnopol'sky, V.T. Voronchev, and P.B. Sazonov, Nucl. Phys. **A417**, 128 (1984).
[23] H. Kanada, T. Kaneko, S. Nagata, and M. Nomoto, Prog. Theor. Phys. **61**, 1327 (1979).
[24] Y. Yamamoto, T. Motoba, H. Himeno, K. Ikeda, and S. Nagata, Prog. Theor. Phys. Suppl. No. 117, 361 (1994); T. Motoba and Y.Yamamoto, Nucl. Phys. **A585**, 29c (1995).
[25] K. Miyagawa, H. Kamada, W. Glöckle, and V. Stoks, Phys. Rev. C **51**, 2905 (1995).
[26] L. Majling, Nucl. Phys. **A585**, 211c (1995).
[27] Y.K. Ho, Phys. Rep. **99**, 1 (1983).